Nuclear Instruments and Methods in Physics Research B 272 (2012) 218–221

Contents lists available at ScienceDirect

Nuclear Instruments and Methods in Physics Research B

journal homepage: www.elsevier.com/locate/nimb

An in situ TEM study of the evolution of Xe bubble populations in UO_2

A. Michel [a,*], C. Sabathier [a], G. Carlot [a], O. Kaïtasov [b], S. Bouffard [c], P. Garcia [a], C. Valot [a]

[a] CEA Cadarache, DEN/DEC/SESC/LLCC, 13108 St Paul Lez Durance, France
[b] CIMAP, CEA – CNRS – ENSICAEN – Université de Caen, 6 boulevard du Maréchal Juin, 14050 Caen cedex 4, France
[c] CSNSM, Université PARIS-SUD 11, bât 104 et 108, 91400 Orsay, France

ARTICLE INFO

Article history:
Available online 1 February 2011

Keywords:
TEM
Irradiation
UO_2
Defects
Precipitation
Xenon

ABSTRACT

Transmission electron microscopy (TEM) experiments were carried out on the JANNUS platform (Joint Accelerators for Nano-science and NUclear Simulation) at CSNSM (Center of Nuclear Spectrometry and Mass Spectrometry) laboratory in Orsay. The experiment was devoted to the study of the evolution of the xenon aggregate population with increasing implantation fluence. A thin UO_2 foil was implanted at fluences ranging from 3×10^{12} to 7×10^{14} at cm^{-2} with 390 keV Xe^{3+} ions at an irradiation temperature of 873 K. The TEM results indicate the presence of nanometer size bubbles above a fluence of 6×10^{12} Xe cm^{-2} and an increase in the bubble number density was observed between 6×10^{12} Xe cm^{-2} and 2×10^{14} Xe cm^{-2}. Above 2×10^{14} Xe cm^{-2}, the number density levels off at $4 \times 10^{23} \pm 0.5 \times 10^{23}$ m^{-3}.

1. Introduction

The lifespan of a nuclear fuel element is limited by the pressure increase within the rod due in part to the release of fission gases (xenon and krypton) and the swelling of the fuel pellet generated by the precipitation of these gases. It is therefore essential to understand and model their behavior in order to develop optimized fuel microstructures that insure improved fuel performance.

Many studies have been carried out in the past on both ion and neutron irradiated UO_2 with the aim of characterizing the development and change in the size distribution of rare gas bubbles. However, handling and characterizing neutron irradiated material is a complex and costly enterprise. Furthermore, neutron irradiations preclude the control of all the relevant experimental conditions (level of damage and damage rate, chemistry of samples, etc.). On the other hand, ion-irradiations provide a cost-effective and efficient means of determining the effect of external or material parameters separately. To our knowledge, no ion-implantation experiments have ever been reported involving the in situ observation of UO_2 thin foils irradiated at temperatures relevant to reactor conditions. We report such a study here.

The experiments are designed as part of a wider program aimed at both improving our knowledge of bubble nucleation mechanisms and particularly the respective role of temperature, radiation damage and foreign atom concentration and generating basic microstructural data that could be used for development or validation of rate diffusion or cluster dynamics models. The JANNUS platform was used since this facility enables the simultaneous high temperature irradiation (IRMA accelerator) and observation (using transmission electron microscopy) of thin foils. We report the results obtained during the first set of experiments carried out on this platform, the objective of which is to generate data relating to the evolution of bubble size distributions as a function of increasing xenon ion fluence in uranium dioxide.

2. Experimental procedure

Polycrystalline UO_2 pellets were polished and then annealed in an Ar-H_2 (5%) gas mixture at 1670 K in order to eliminate the damage induced by polishing and to guarantee the stoichiometry of the samples. Mechanical thinning by polishing with a tripod followed by chemical etching was employed to obtain the thin foils [1]. The UO_2 thin foil was then placed in the double tilt sample holder equipped with an annealing device. The transmission electron microscope (FEI Tecnai G2 Twin 20) used operates at 200 kV and is equipped with a CCD camera. The energy of the Xe^{3+} ions selected is 390 keV in order to guarantee that the energy of all impinging ions is deposited within the foil and that a majority of ions is located in the zone that can be observed using TEM (between 0 and 100 nm from the sample surface). The implantation depth estimated with SRIM [2] is about 70 nm. With a constant flux of 5×10^{11} Xe cm^{-2} s^{-1} it was possible to carry out observations over a wide range of fluences between 3×10^{12} and 7×10^{14} Xe cm^{-2} (3×10^{12}; 6×10^{12}; 10^{13}; 1.3×10^{13}; 1.7×10^{13}; 3×10^{13};

* Corresponding author. Tel.: +33 4 4225 5130; fax: +33 4 4225 3285.
E-mail addresses: amelie.michel@cea.fr (A. Michel), catherine.sabathier@cea.fr (C. Sabathier), gaelle.carlot@cea.fr (G. Carlot), kaitasov@csnsm.in2p3.fr (O. Kaïtasov), serge.bouffard@cea.fr (S. Bouffard), philippe.garcia@cea.fr (P. Garcia), carole.valot@cea.fr (C. Valot).

0168-583X/$ - see front matter © 2011 Elsevier B.V. All rights reserved.
doi:10.1016/j.nimb.2011.01.069

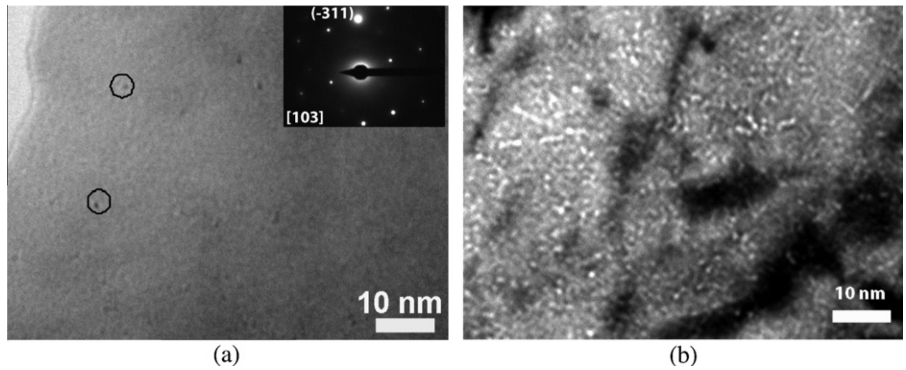

Fig. 1. TEM images of UO_2 thin foils implanted with 390 keV Xe ions at 870 K and at a fluence of (a) 6×10^{12} Xe cm^{-2} in overfocused beam conditions: dark spots and (b) 7×10^{14} Xe cm^{-2} in underfocused beam conditions: bright spots.

Table 1
Average diameter and number density of the bubble population as a function of fluence.

Fluence (at cm^{-2})	Number density ($\times 10^{23}$ m^{-3})		Diameter (nm)	
	Value	σ_{theo}	Value	σ_{theo}
6×10^{12}	0.20	0.26	0.87	0.14
1×10^{13}	0.46	0.37	0.88	0.16
1.3×10^{13}	0.63	0.50	0.90	0.14
1.7×10^{13}	0.75	0.58	0.83	0.11
3×10^{13}	1.79	0.67	0.70	0.12
4×10^{13}	3.18	1.20	0.78	0.12
4.5×10^{13}	4.49	0.71	0.69	0.11
5×10^{13}	2.33	0.70	0.69	0.10
6×10^{13}	2.16	0.66	1.03	0.16
8×10^{13}	3.69	1.16	0.88	0.14
2×10^{14}	4.40	1.32	0.84	0.13
7×10^{14}	3.30	0.94	1.04	0.20

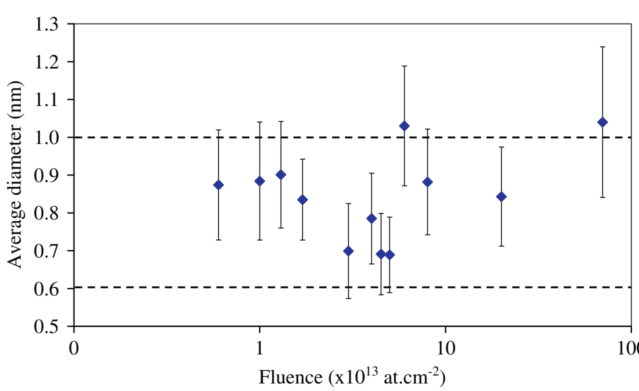

Fig. 2. Changes in the average bubble diameter as a function of fluence for fluences ranging between 3×10^{12} and 7×10^{14} Xe cm^{-2}.

4×10^{13}; 4.5×10^{13}; 5×10^{13}; 6×10^{13}; 8×10^{13}; 2×10^{14}; 7×10^{14} Xe cm^{-2}) corresponding to a maximum gas concentration ranging between 4×10^{-4} at.% and 0.1 at.%. The flux was chosen to guarantee limited heating of the thin foil and the parameters of the beam were adjusted to produce a homogeneous flux. Implantations were performed at a temperature of 870 K. After each implantation, TEM characterizations were carried out at room temperature. The images were systematically recorded in under and over focused beam conditions to reveal the presence of xenon bubbles.

3. Results

At the lowest fluence, 3×10^{12} Xe cm^{-2}, it is impossible to detect the presence of xenon bubbles on the images. For fluences greater than 6×10^{12} Xe cm^{-2}, xenon bubbles are seen. An image using over focused beam conditions at a fluence of 6×10^{12} Xe cm^{-2} is given in Fig. 1(a). An image obtained at the fluence 7×10^{14} Xe cm^{-2} is shown in Fig. 1(b). At each fluence, the bubble populations were characterized based on an analysis of the TEM images obtained under conditions where the electron beam was parallel to the axis [1 0 3] as illustrated by the diffraction pattern given in Fig. 1(a). The large number of counted and measured bubbles enabled us to determine accurate standard deviations for both bubble diameters and densities. All the results are given for a confidence interval of 68%.

The average bubble diameter is given for each fluence greater than 6×10^{12} Xe cm^{-2}. The results are gathered in Table 1 and illustrated in Fig. 2. They show that the average bubble diameter is virtually independent of fluence, within the experimental uncertainty, at least up to 2×10^{14} Xe cm^{-2} and is equal to 0.8 ± 0.2 nm. Fig. 3(a) represents the size distribution of the bubbles at a fluence of 8×10^{13} Xe cm^{-2}: it follows a Gaussian distribution as do all other bubble size distributions other than the one corresponding to the highest fluence. Indeed for a fluence of 7×10^{14} Xe cm^{-2},

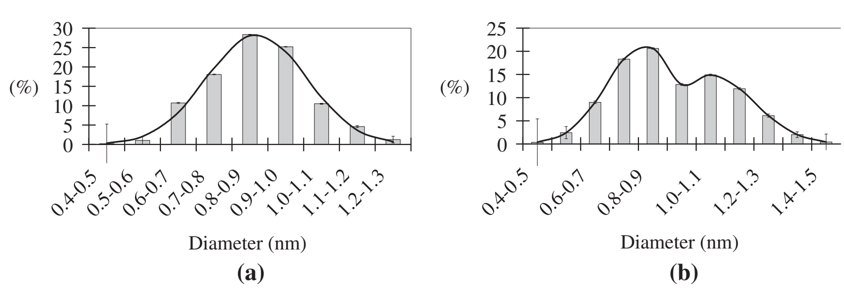

Fig. 3. Size distribution of bubbles for implantations at fluences of 8×10^{13} (a) and 7×10^{14} Xe cm^{-2} (b).